LEIDEN UNIVERSITY

Study of BCG-Substracted Images of Nearby Clusters

by

Juan Manuel Espejo Salcedo

Advisor:

Dr. Henk Hoekstra

Natural Sciences Faculty
Sterrenwacht

March 2017

"Not only is the Universe stranger than we think, it is stranger than we can think.."

Werner Heisenberg

Abstract

Natural Sciences Faculty
Sterrenwacht

(This is just a simple draft taken from the original idea) We have obtained deep imaging data for a sample of low redshift massive clusters. The light from the BGC overwhelms the images from background galaxies and faint cluster members in the cluster core, and needs to be carefully subtracted. This is expected to reveal background galaxies that are strongly lensed. Identifying such systems allows for unique follow-up studies. Also the number density of faint cluster members may tell us something about the dynamical state of the cluster and how BGCs form. The aim of this project is to model the BCG light and search for strong lensing candidates and study the properties of faint cluster members in the core..

Acknowledgements

I would like to thank ...

Contents

List of Figures

List of Tables

Dedicated to my parents, whose love and support are my biggest motivation...

Chapter 1

Introduction

-Science case:

Stellar mass to light ratio and Stellar populations in the BCGs (ac'a es donde se deben hacer las citaciones mas importantes)

-Galaxy Clusters-

IMF is a very fundamental and important quantity in the study of stellar systems because it constraints the physicis of star formation but also because it allows us to infer stellar masses through observed luminosities.

the correct use of an IMF in the context of gravitational lensing on masssive objects like early type galaxies in galaxy clusters can help us constraint the ammount of stellar mass and thus also infer the ammount of dark matter in these systems.

Studying the ammount of dark matter contribution, one could in principle make a good estimation of the stellar mass'to'light ratio.

For galaxies that are far away, it is impossible to make star counts, for this reason, the mass to light ratio of the stellar population provides a simple constraint on the IMF (Russell J. Smith and John R. Lucey)

Strong gravitational lensing of background galaxies provides a useful method to determinemasses in elliptical galaxies, since it is difficult to constrint the IMF via M/L

massive galaxies - salpeter is a good IMF

A Koupra IMF finds a value of gamma of around 4 for the mass to light ratio. (R. J. Smith 2014)

DM fraction in comparison with the IMF

Studying the matter distribution given by strong gravitational lensing can give us informarion about the iMF of the BCGs

percentage of dark matter will allow me to define the IMF more precisely. I want to see what fraction of the mass, what fraction of the surface density is stars

strong lensing at different radii is usefull.

if I got to certeain radius I will have more dark matter, becaue light drops quickly.

basically find how much dark matter and hoy many stars are there in the profile

Chapter 2

Theoretical Framework

Tyter.

2.1 Galaxy Clusters

Glas.

dwarf stars contribute very little to the integrated light from an old stellar population (Smith 2015)

Galaxy clusters contain a population of stars gravitationally unbound to individual galaxies, yet still bound to the clusters overall gravitational potential, created by the stripping of stars from galaxies during interactions and mergers

FIGURE 2.1: G

Quoted (need to change this):The image of galaxy cluster MACS J1206.2-0847 (or MACS 1206) is part of a broad survey with NASA Hubble Space Telescope.The distorted shapes in the cluster are distant galaxies from which the light is bent by the gravitational pull of an invisible material called dark matter within the cluster of galaxies. This cluster is an early target in a survey that will allow astronomers to construct the most detailed dark matter maps of more galaxy clusters than ever before.These maps are being used to test previous, but surprising, results that suggest that dark matter is more densely packed inside clusters than some models predict. This might mean that galaxy cluster assembly began earlier than commonly thought.

Scientists are planning to observe a total of 25 galaxy clusters under a project called CLASH (Cluster Lensing and Supernova survey with Hubble).One of the first objects observed for the new census is the galaxy cluster MACS J1206.2-0847. This conglomeration of galaxies is one of the most massive structures in the universe, and its gigantic gravitational pull causes stunning gravitational lensing. MACS 1206 lies 4 billion light-years from Earth. In addition to curving of light, gravitational lensing often produces double images of the same galaxy. In the new observation of cluster MACS J1206.2-0847, astronomers counted 47 multiple images of 12 newly identified galaxies.The era when the first clusters formed is not precisely known, but is estimated to be at least 9

billion years ago and possibly as far back as 12 billion years ago. If most of the clusters in the CLASH survey are found to have excessively high accumulations of dark matter in their central cores, then it may yield new clues to the early stages in the origin of structure in the universe.

2.2 Gravitational Lensing

At small radii, stars dominate the lensing mass, so that lensing provides a direct probe of the stellar mas to light ratio, with only small corrections needed for dark matter.

In the paper of Russell Smith (a giant elliptical galaxy with a lightweight initial mass funciton) they find a stellar mass to light ratio of 3.01 plus minus 0.25

Modelling the lensing configuration provides the total projection mass within an aperture.

NFW profile for dark matter that is basically the dynamical mass of the cluster

let's take the case of ABELL1068, it's magnitude in U is 21.94, in I is 18.46, in g is 20.09, in r is 19.5, also $M_{200} = 4.3 \times 10^{14} M_{\odot}$

The bolometric luminosity of Abell1068 is $10^4$4erg/s that in solar luminosities is $1.9 \times 10^{12} L_s ol$, this gives an effective brightness of $2^2 M_{\odot}/kpc^2$.

the distance to the galaxy is 591.42857 Mpc

salpeter mass function is $n(M) \propto M^{-2.3}$

de Vaucouleurs law for the surface brightness distribution in giant elliptical galaxies is:

$$I(R) = I_e e^{-b\left[(R/R_e)^{1/4}-1\right]} \tag{2.1}$$

where $b = 7.67$ and I_e is the effective brightness which is basically the brightness at the effective radius R_e

From the paper of Lokas and Mamon, for constant mass-light-ratio we have $\Sigma_M(R) = \Gamma I(R)$ where I is the surface brightness.

the NFW density profile is

$$\rho(r) = \frac{\delta_c \rho_c}{(r/r_s)(1 + r/r_s)^2} \tag{2.2}$$

where the characteristic overdensity is:

$$\delta_c = \frac{200}{3} \frac{c^3}{\ln(1+c) - c/(1+c)} \tag{2.3}$$

from Munoz cuartas et. al. we see that the concentration parameter depends on the mass and the redshift as we see in the following plot:

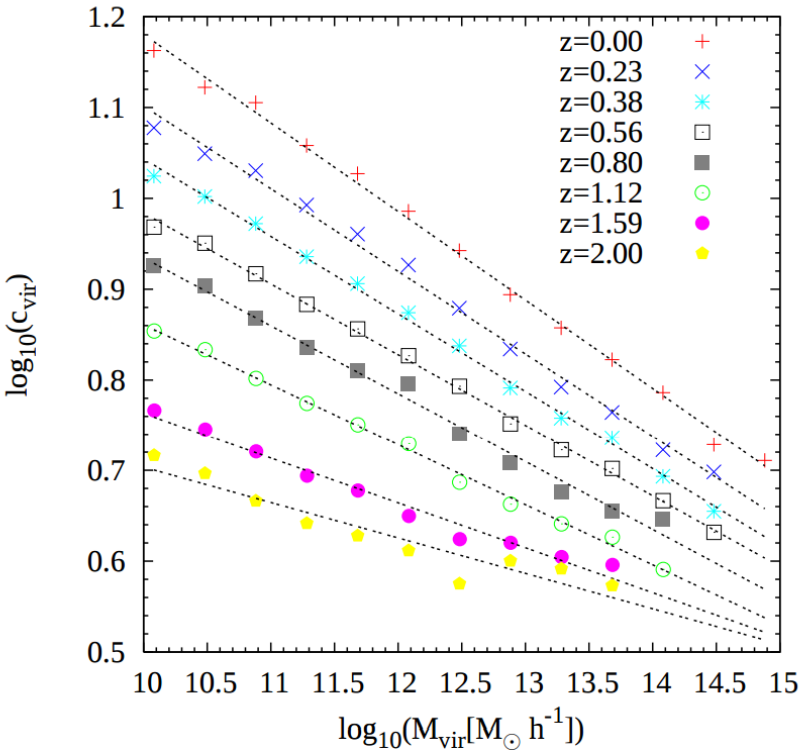

FIGURE 2.2: G

$c = r_{200}/r_s$

The concentration parameter c is strongly correlated with Hubble type, c=2.6 separating early from late-type galaxies. Those galaxies with concentration incides c¿2.6 are early-type galaxies reflecting the fact that the light is more concentrated towards their centres

From Dutton and Maccio 2014 we get the following image for the concentration parameter:

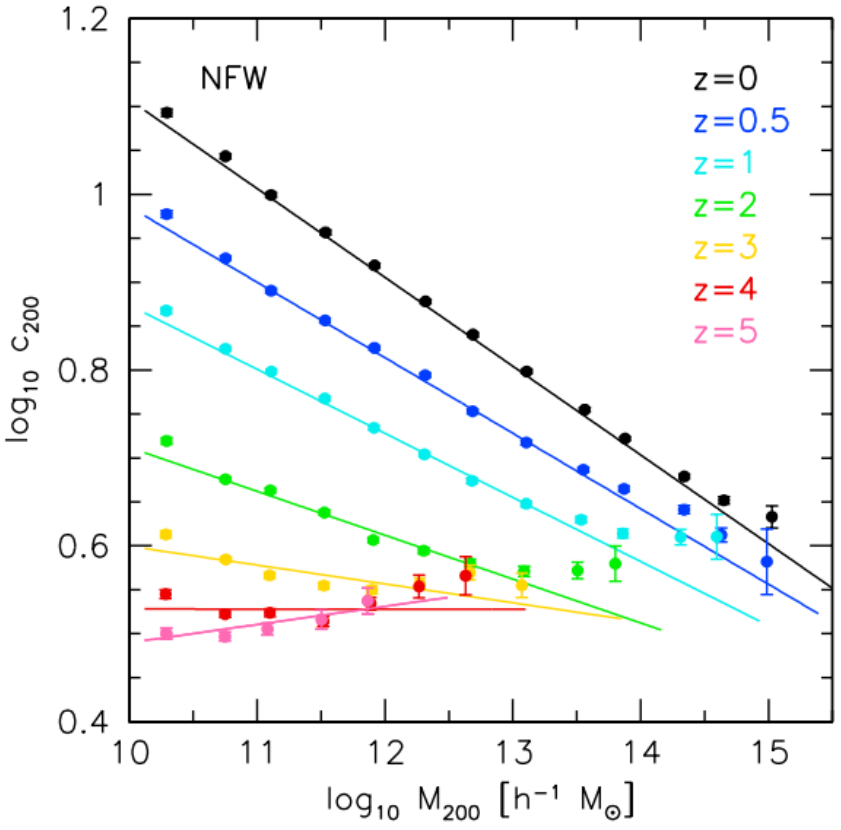

FIGURE 2.3: G

The surface mass density is given by:

$$\Sigma_{\rm NFW}(x) = \begin{cases} \frac{2r_s\delta_c\rho_c}{(x^2-1)}\left[1-\frac{2}{\sqrt{1-x^2}}\operatorname{arctanh}\sqrt{\frac{1-x}{1+x}}\right](x<1) & (x<1) \\ \frac{2r_s\delta_c\rho_c}{3}(x=1) & (x=1) \\ \frac{2r_s\delta_c\rho_c}{(x^2-1)}\left[1-\frac{2}{\sqrt{x^2-1}}\arctan\sqrt{\frac{x-1}{1+x}}\right](x<1) & (x>1) \end{cases} \tag{2.4}$$

then the concentration parameter for ABELL1068 is about 7.9 supposing a mass of the galaxy of $10^{12.5}M_{\odot}$

so from the critical density:

$$\rho_c = \frac{3H^2(z)}{8\pi G} \tag{2.5}$$

the critical density would be: 2×10^{-26} in SI units so in Msol/pc3 it is 2.9×10^{-7}

$H(z) = H_0(1 + \Omega z)^{3/2}$

the Hubble parameter at z=0.138 is H(z)=85.6

delta c is 25315 (dimensionless)

The characteristic radius is given by $r_{1/2} = 1.34R_e$

The mass to light ratio is $\gamma = 4$

Here the surface mass density for both the stellar content and the NFW profile:

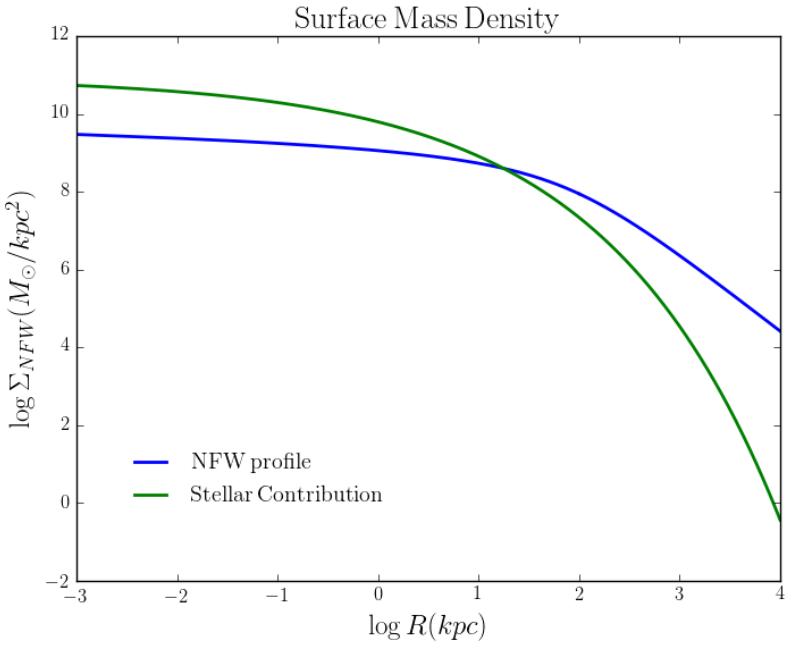

FIGURE 2.4: G

But we are more interested in the enclosed mass which can be done by integrating the surface mass density:

$$M(R) = \int_0^R 2\pi R\Sigma(R)dR \tag{2.6}$$

And we can recover our luminosity by integrating the surface brightness profile like this:

$$L = \int_0^R 2\pi RI(R)dR \tag{2.7}$$

That should give us a value comparable to the one found using Faber-Jackson relation: $L = C \times \sigma^4$

And the plot for the enclosed mass is:

Mass.png Mass.png Mass.png Mass.png Mass.png Mass.png Mass.png Mass.png

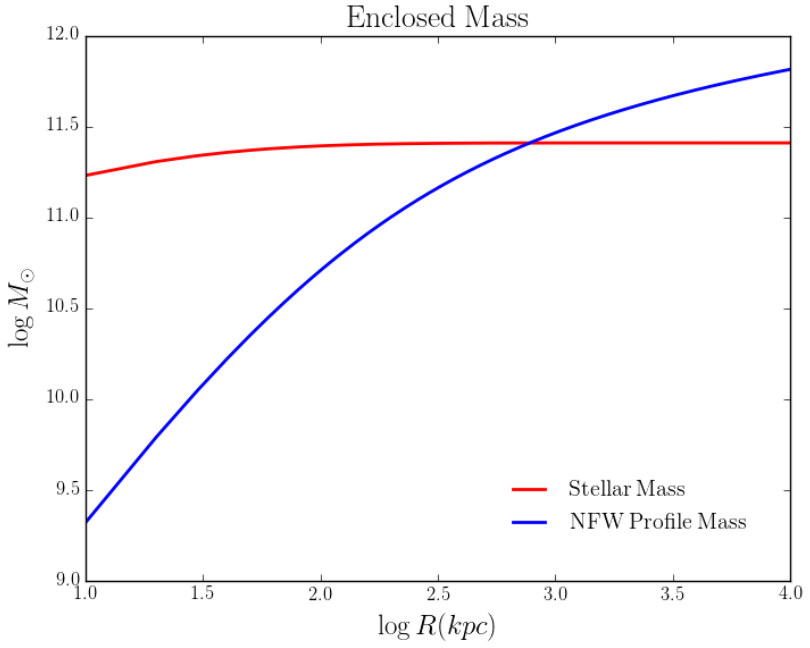

Mass.png

FIGURE 2.5: G

The radial dependence on the shear is:

$$\gamma_{\rm NFW}(x) = \begin{cases} \frac{r_s \delta_c \rho_c}{\Sigma_c} g_<(x) & (x < 1) \\ \frac{r_s \delta_c \rho_c}{\Sigma_c} \left[\frac{10}{3} + 4 \ln\left(\frac{1}{2}\right)\right] & (x = 1) \\ \frac{r_s \delta_c \rho_c}{\Sigma_c} g_>(x) & (x > 1) \end{cases} \tag{2.8}$$

where:

$$g_<(x) = \frac{8 \operatorname{arctanh} \sqrt{\frac{1-x}{1+x}}}{x^2 \sqrt{1-x^2}} + \frac{4}{x^2} \ln\left(\frac{x}{2}\right) - \frac{2}{(x^2-1)} + \frac{4 \operatorname{arctanh} \sqrt{\frac{1-x}{1+x}}}{(x^2-1)\,(1-x^2)^{1/2}} \tag{2.9}$$

$$g_<(x) = \frac{8 \arctan \sqrt{\frac{x-1}{1+x}}}{x^2 \sqrt{x^2-1}} + \frac{4}{x^2} \ln\left(\frac{x}{2}\right) - \frac{2}{(x^2-1)} + \frac{4 \arctan \sqrt{\frac{x-1}{1+x}}}{(x^2-1)^{3/2}} \tag{2.10}$$

and with the critical surface mass density:

$$\Sigma_c \equiv \frac{c^2}{4\pi G}\frac{D_s}{D_d D_{ds}} \tag{2.11}$$

these equations come from the paper Wright and Brainerd 1999

the plot of the shear dependence on the radius is:

dependence on radius.png dependence on radius.png dependence on radius.png dependence on radius.png dependence on radius.png dependence on radius.png dependence on radius.png dependence on radius.png dependence on radius.png

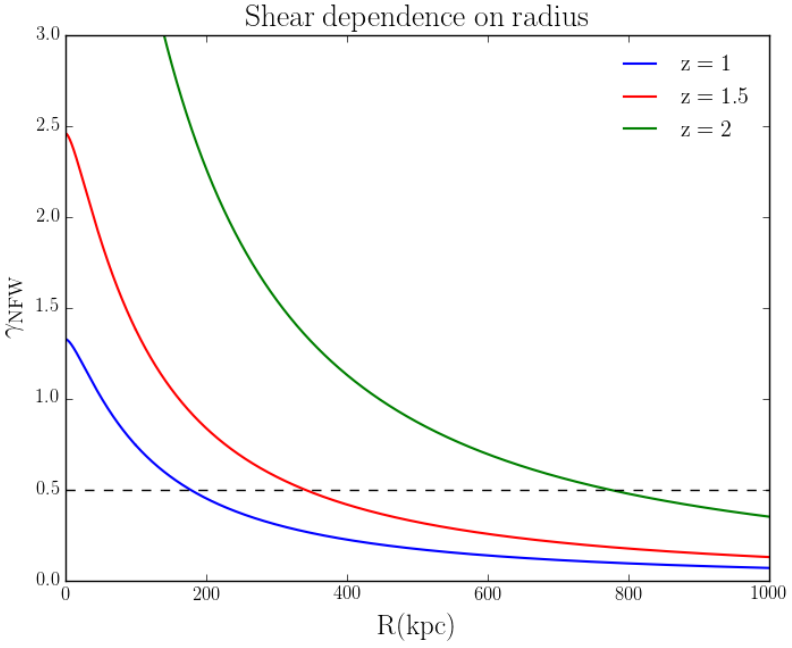

FIGURE 2.6: G

The magnification tensor is:

$$\frac{\partial\beta}{\partial\theta} = \delta_{ij} - \frac{\partial^2\psi}{\partial\theta_i\partial\theta_j} = \begin{pmatrix} 1-\kappa-\gamma_1 & -\gamma_2 \\ -\gamma_2 & 1-\kappa+\gamma_1 \end{pmatrix} \tag{2.12}$$

The total magnification μ is given by the determinant of the magnification tensor:

$$\mu = \frac{1}{(1-\kappa)^2 - \gamma_1^2 - \gamma_2^2} \tag{2.13}$$

Where κ is the convergence that determines the magnification and γ_1 and γ_2 are the shear components that determine the distorsion of the background objects.

2.3 IMF in BCGs

For stars, measurements of the luminosity function can be used to derive the Initial Mass Function (IMF). For galaxies, this is more difficult because Mass to light ratio (M/L) of the stellar population depends upon the star formation history of the galaxy.

bulges have heavier IMFs than disks

Several recent studies have presented evidence for "heavyweight" IMFs in giant ellipticals, with a mass-to-light-ratio twice that of a Milky Way like IMF.

Chapter 3

Observational Procedures

the full description of the survey is in: D. J. Sand et. al. 2011

MegaCam wide field imager on the CFHT (Canada-France-Hawii Telescope). The cluster sample consisted of 101 clusters within the range of redshifts from 0.05 ¡ z¡ 0.55

58 clusters from the MENEACs (Multi-Epoch nearby cluster survey)

The meneacs clusters represent all clusters in the BAX X-ray cluster database that are observable fof the CFHT

the redshifts of the clusters as given by C. Bildfell et. al. 2012

G, U, I and R images

3.1 Sextractor

Stars and selection of galaxies

Color magnitude diagram for A1068

Cluster	z	$\sigma(km/s)$	$d(Mpc)$	$\theta_E(")$
A1033	0.126	762		14.6155
A1068*	0.138	740		13.5945
A1132	0.136	727		13.1515
A119*	0.044	875		21.0798
A1413*	0.143	881		19.1569
A1650	0.084	720		13.6758
A1651	0.085	903		21.4876
A1795	0.062	778		16.3514
A2029*	0.077	1152		35.2776
A2050	0.118	854		18.5258
A2055	0.102	697		12.5642
A2064	0.108	675		11.7048
A2065*	0.073	1095		32.0110
A2069	0.116	966		23.7574
A2142*	0.091	1086		30.8756
A2319*	0.056	1101		32.9563
A2420	0.085	800		16.8653
A2440	0.091	766		15.3608
A2597	0.085	682		12.2569
A2627	0.126	800		16.1096
A2703	0.114	800		16.3307
A399	0.072	800		17.1049
A553	0.066	800		17.2155
A655*	0.127	800		16.0911
A754*	0.054	800		17.4367
A763	0.085	800		16.8653
A795	0.136	800		15.9252
A85*	0.055	800		17.4182
A961	0.124	800		16.1464
A990	0.144	800		15.7778

TABLE 3.1: My caption

mag.png mag.png mag.png mag.png mag.png mag.png mag.png mag.png mag.png

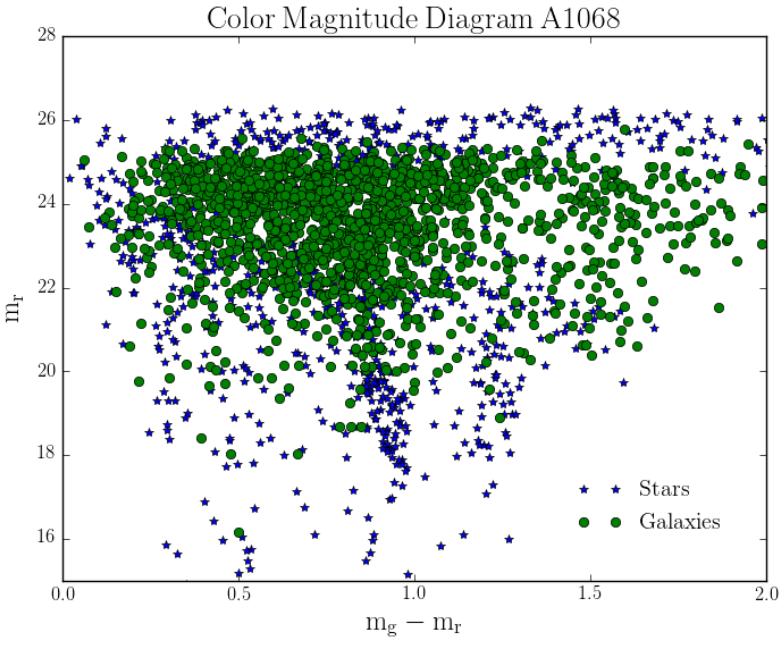

FIGURE 3.1: G

Mag vs flux rad to discriminate

vs flux rad.png vs flux rad.png vs flux rad.png vs flux rad.png vs flux rad.png vs flux rad.png vs flux rad.png vs flux rad.png vs flux rad.png

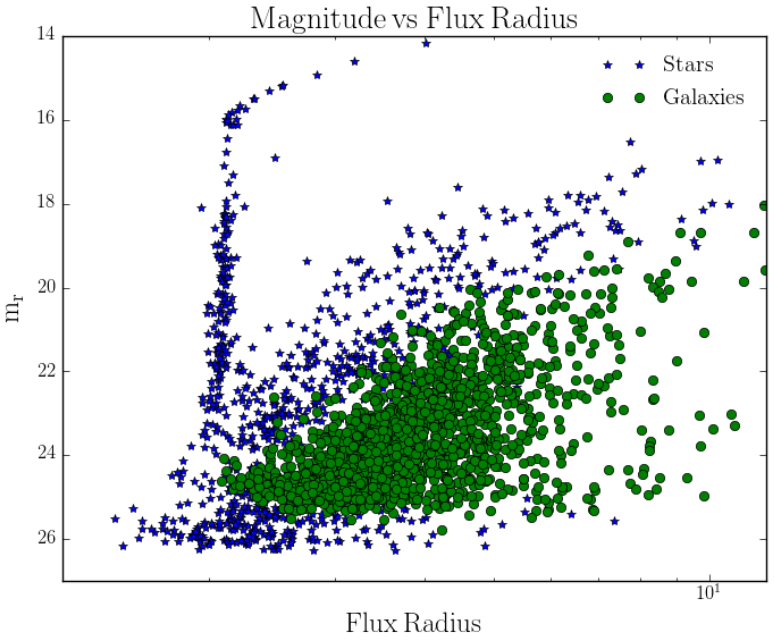

FIGURE 3.2: G

3.2 Galfit

The parameters C0, B1, B2, F1, F2, etc. listed below are hidden from the user unless he/she explicitly requests them. These can be tagged on to the end of any previous components except, of course, the PSF and the sky – although galfit won't bar you from doing so, and will just ignore them. Note that a Fourier or Bending mode amplitude of exactly 0 will cause GALFIT to crash because the derivative image GALFIT computes internally will be entirely 0. If a Fourier or Bending amplitude is set to 0 initially GALFIT will reset it to a value of 0.01. To prevent GALFIT from doing so, one can set it to any other value.

Bending modes B1) 0.07 1 Bending mode 1 (shear) B2) 0.01 1 Bending mode 2 (banana shape) B3) 0.03 1 Bending mode 3 (S-shape)

Azimuthal fourier modes F1) 0.07 30.1 1 1 Az. Fourier mode 1, amplitude and phase angle F2) 0.01 10.5 1 1 Az. Fourier mode 2, amplitude and phase angle F6) 0.03 10.5 1 1 Az. Fourier mode 6, amplitude and phase angle F10) 0.08 20.5 1 1 Az. Fourier mode 10, amplitude and phase angle F20) 0.01 23.5 1 1 Az. Fourier mode 20, amplitude and phase angle

Traditional Diskyness/Boxyness parameter c C0) 0.1 0 traditional diskyness(-)/boxyness(+)

3.3 Color images

In er.

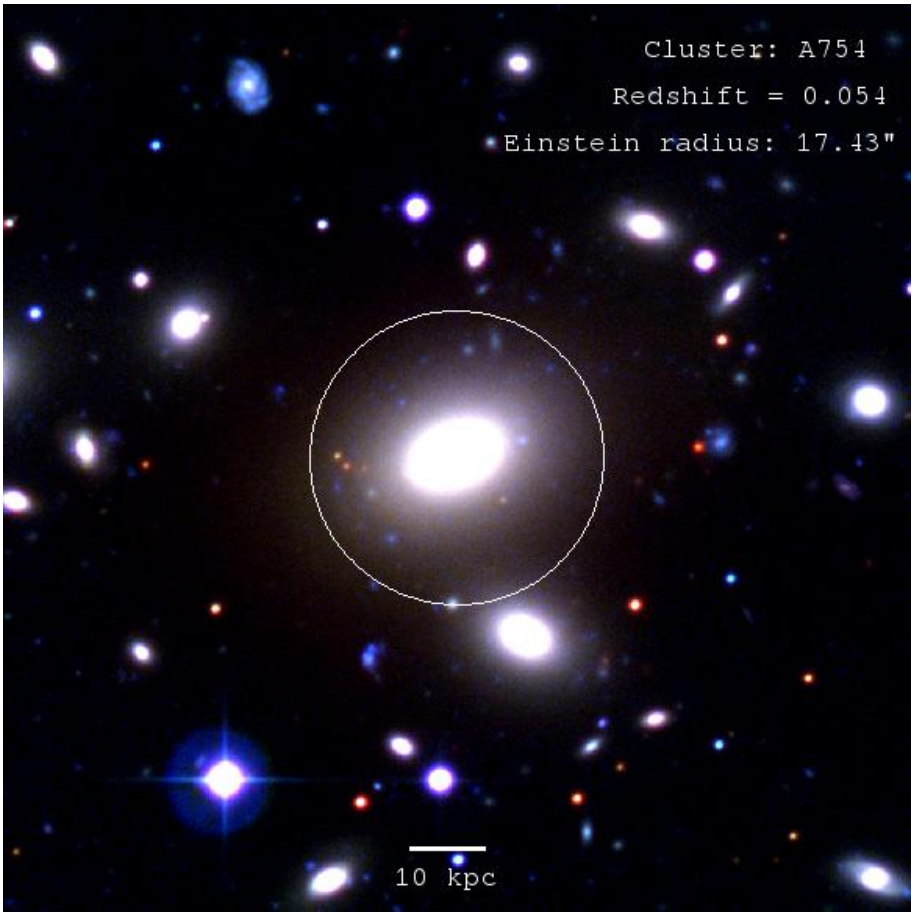

FIGURE 3.3: G

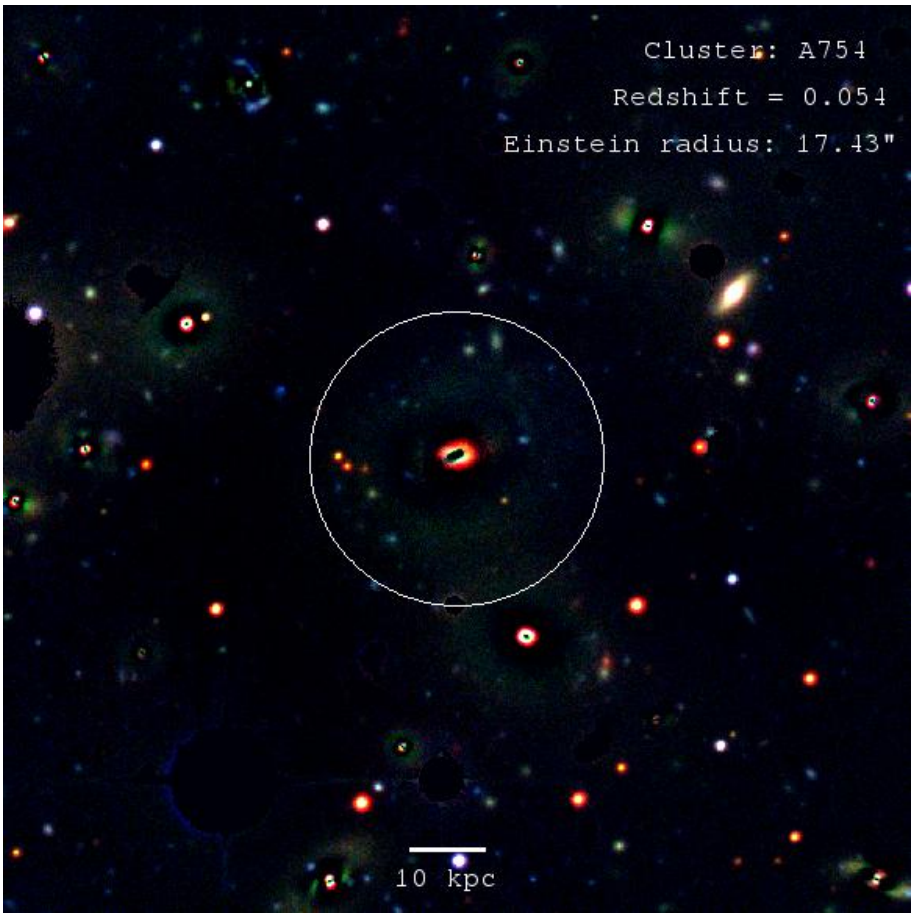

FIGURE 3.4: G

3.4 Photometric Redshift

(using as reference Benitez, Narciso 2000)

Chapter 4

Study of images

We ter.

Chapter 5

Conclusions

Thes.

Bibliography

[1] Treu, Tommaso. 2010 *Strong Lensing by Galaxies*. Annu. Rev. Astron. Astrophysics. 2010. 48:87-125.

[2] R. F. J. Van der Burg et. al. 2015 *Evidence for the inside-out growth of the stellar mass distribution in galaxy clusters since z1̃*. preprint arXiv:1412.2137v2.

[3] Binney J., Tremaine S. *Galactic Dynamics*. Princeton University Press, 1994.

[4] C. O. Wright & Teresa G. Brainerd, Teresa. 1999 *Gravitational Lensing by NFW halos*. preprint arXiv:astro-ph/9908213v1.

[5] Smith, Russell. 2014 *Variations in the initial mass function in early-type galaxies: a critical comparison between dynamical and spectroscopic results*. MNRASL 443, L69-L73 (2014).

[6] C. Bildfell et. al. 2012 *Evolution of the red sequence giant to dwarf ratio in galaxy clusters out to z0̃.5*. MNRAS 425, 204-221 (2012).

[7] Smith, Russell & Lucey, John. 2013 *A giant elliptical galaxy with a lightweight initial mass function*. MNRAS 000, 1-14 (2013).

[8] R. J. Smith et. al. 2015 *The IMF-sensitive 1.14-μm Na I doublet in early-type galaxies*. MNRAS 000, 1-14 (2013).

[9] C. Sifon et. al. 2015 *Constraints on the alignment of galaxies in galaxy clusters from 1̃4000 spectroscopic members*. A&A 575, A48 (2015).

[10] S. M. Adams et. al. 2012 *The environmental dependence of the incidence of galactic tidal features*. The Astrophysical Journal, 144:128(11pp) (2012).

[11] D. J. Sand et. al. 2011 *Intracluster supernovae in the multi-epoch nearby cluster survey*. The Astrophysical Journal, 729:142 (13pp) (2011).

[12] J. C. Muñoz Cuartas et. al. 2010 *The redshift evolution of ΛCDM halo parameters: concentration, spin and shape*. MNRAS, 000,1-11 (2010).